

Partial fusion of a weakly bound projectile with heavy target at energies above the Coulomb barrier

Z.H. Liu^{1,a}, C. Signorini², M. Mazzocco², M. Ruan¹, H.Q. Zhang¹, T. Glodariu^{2,b}, Y.W. Wu¹, F. Soramel³, C.J. Lin¹, and F. Yang¹

¹ China Institute of Atomic Energy, P.O. Box 275(10), Beijing 102413, PRC

² Physics Department of the University and INFN, Via Marzolo 8, 35131, Padova, Italy

³ Physics Department of the University and INFN, Udine, Via delle Scienze 208, 33100, Udine, Italy

Received: 21 July 2004 / Revised version: 20 June 2005 /

Published online: 28 October 2005 – © Società Italiana di Fisica / Springer-Verlag 2005

Communicated by W. Henning

Abstract. Partial-fusion cross-sections for the systems ${}^6\text{Li} + {}^{208}\text{Pb}$, ${}^9\text{Be} + {}^{209}\text{Bi}$ have been determined. The effect of breakup on fusion for weakly bound projectiles ${}^6\text{Li}$ and ${}^9\text{Be}$ incident on ${}^{208}\text{Pb}$ or ${}^{209}\text{Bi}$ targets has been discussed comparing experimental fusion cross-section excitation functions to those evaluated with a semi-classical approach. It is shown that complete fusion of a weakly bound projectile with heavy target is reduced, whereas the breakup process has very little influence on the total-fusion cross-section for some of the studied systems at energies above the Coulomb barrier.

PACS. 25.70.Ji Fusion and fusion-fission reactions – 25.70.Mn Projectile and target fragmentation

1 Introduction

The availability of Radioactive Ion Beams (RIBs) has opened many new perspectives to nuclear physics studies. One example is the behavior of light-mass RIBs (either weakly bound or with a halo structure) in the fusion process. In fact, during the interaction with a heavy stable target these nuclei drive the process towards different paths: The two nuclei undergo a complete-fusion (CF) process, alternatively the radioactive nucleus breaks in lighter nuclei (breakup) and one of the fragments is captured by the target nucleus resulting in an incomplete- or partial-fusion (ICF) process. Several theoretical [1–6] and experimental [7–17] works have been published on this subject. From the theoretical point of view two different conflicting scenarios have been foreseen; one [5] predicts a fusion enhancement with respect to reactions involving stable nuclei, the other [1–4] predicts a fusion cross-section suppression due to the reaction flux lost in the breakup channel. Recently, Hagino *et al.* [6] performed an improved coupled-channels calculation with the aim of reconciling the two conflicting scenarios; they predicted a complete-fusion cross-section enhancement at energies below the Coulomb barrier and a suppression at energies above the

Coulomb barrier. These different theoretical predictions call for precise and reliable measurements as a watershed among various theories. To this goal, many experiments have been performed with halo (${}^6\text{He}$, ${}^{11}\text{Be}$) [7–11] and weakly bound (${}^6\text{Li}$, ${}^9\text{Be}$, ${}^{17}\text{F}$) [12–17] projectiles. The experimental results obtained with ${}^6\text{Li}$ and ${}^9\text{Be}$ projectiles have been compared to different theoretical predictions and, in any case, despite the reference model, a sizable reduction of the complete-fusion cross-section has been observed. The aim of this paper is to analyze the data for ${}^6\text{Li}$ and ${}^9\text{Be}$ pointing out the relation between partial and complete fusion at energies above the Coulomb barrier.

2 Incomplete-fusion data

Our first step has been to examine the four systems ${}^6\text{Li}$, ${}^9\text{Be} + {}^{208}\text{Pb}$, ${}^{209}\text{Bi}$ to get information on the ICF cross-section. For the systems ${}^6\text{Li} + {}^{209}\text{Bi}$ [13] and ${}^9\text{Be} + {}^{208}\text{Pb}$ [14] we had already an ICF cross-section measurement, while for the systems ${}^6\text{Li} + {}^{208}\text{Pb}$ and ${}^9\text{Be} + {}^{209}\text{Bi}$ the ICF cross-sections were deduced from a new analysis of data collected during previous experiments. In the following we define the total-fusion cross-section (σ_{fus}) as the sum of complete-fusion cross-section (σ_{CF}) and incomplete-fusion cross-section (σ_{ICF}), *i.e.* $\sigma_{\text{fus}} = \sigma_{\text{CF}} + \sigma_{\text{ICF}}$.

^a e-mail: zhliu@iris.ciae.ac.cn

^b On leave from the National Institute of Physics and Nuclear Engineering, P.O. Box MG-6, Bucharest - Magurele, Romania.

Table 1. Incomplete-fusion cross-sections for the system ${}^6\text{Li} + {}^{208}\text{Pb}$. The quoted errors are, as in ref. [18] (table III), only statistical. The absolute accuracy is around 5%.

$E_{c.m.}$ (MeV)	$\sigma_{ICF}^{exp.}$ (mb)	$\Delta\sigma_{ICF}^{exp.}$ (mb)
30.1	198.6	1.4
32.1	321.8	2.0
34.0	422.9	4.1
37.9	616.6	7.9

2.1 The ${}^6\text{Li} + {}^{208}\text{Pb}$ system

In this experiment, described in more detail in [18], the light charged particles were detected in the $8\pi\text{LP}$ setup of LNL [19] using 126 two-stage telescopes, Si- ΔE and CsI(Tl)- E_{res} arranged all around the target in a spherical geometry. The collected data allowed to extract the differential and total cross-sections for α , d , and p (σ_α , σ_d , σ_p) production at four beam energies, as well as the cross-section for α - d and α - p coincidences ($\sigma_{\alpha-d}$, $\sigma_{\alpha-p}$). Combining the cross-sections and assuming that

- the α -particle never breaks since it has a large binding energy,
- the evaporation cross-sections for d and α from the compound nucleus are, as predicted from the PACE4 code, negligible if compared to the measured cross-sections,
- the α , d and p transfer cross-sections are negligible, too, (FRESCO code),

we could extract α and d capture cross-sections:

$$\sigma_d^{capture} = \sigma_\alpha - \sigma_{\alpha-d} - \sigma_{\alpha-p}, \quad (1)$$

$$\sigma_\alpha^{capture} = \sigma_d - \sigma_{\alpha-d} - \sigma_{\alpha-p}. \quad (2)$$

The sum of the two capture cross-sections gives the ICF cross-sections of table 1 and fig. 1a.

2.2 The ${}^9\text{Be} + {}^{209}\text{Bi}$ system

In this experiment [15] the charged particles were detected using $E(\text{Si})$ detectors placed at backward angles. The α -particles emitted in the decay of the various evaporation residues produced in the reaction were identified through their characteristic decay energies. The only ICF channel we could clearly identify is the one that, following the fusion of ${}^4,{}^5\text{He}$ (${}^9\text{Be}$ breakup fragments) with the ${}^{209}\text{Bi}$ target, populates the ${}^{212}\text{At}$ residual nucleus after $1n(2n)$ evaporation following ${}^4\text{He}({}^5\text{He})$ incomplete fusion. These cross-sections data are given in table 2 and plotted in fig. 1b together with σ_{CF} data. We underline that these data, far from exhausting the σ_{ICF} of the ${}^9\text{Be} + {}^{209}\text{Bi}$ system, most likely do represent the largest contribution to σ_{ICF} , as already found for the system ${}^9\text{Be} + {}^{208}\text{Pb}$ [14]. We can conclude that for ${}^9\text{Be} + {}^{209}\text{Bi}$ the σ_{ICF} data we have deduced are 30–40% lower than the real σ_{ICF} . The ${}^6\text{Li} + {}^{208}\text{Pb}$ ICF cross-section is large, while for the ${}^9\text{Be} + {}^{209}\text{Bi}$ system it is smaller but not negligible.

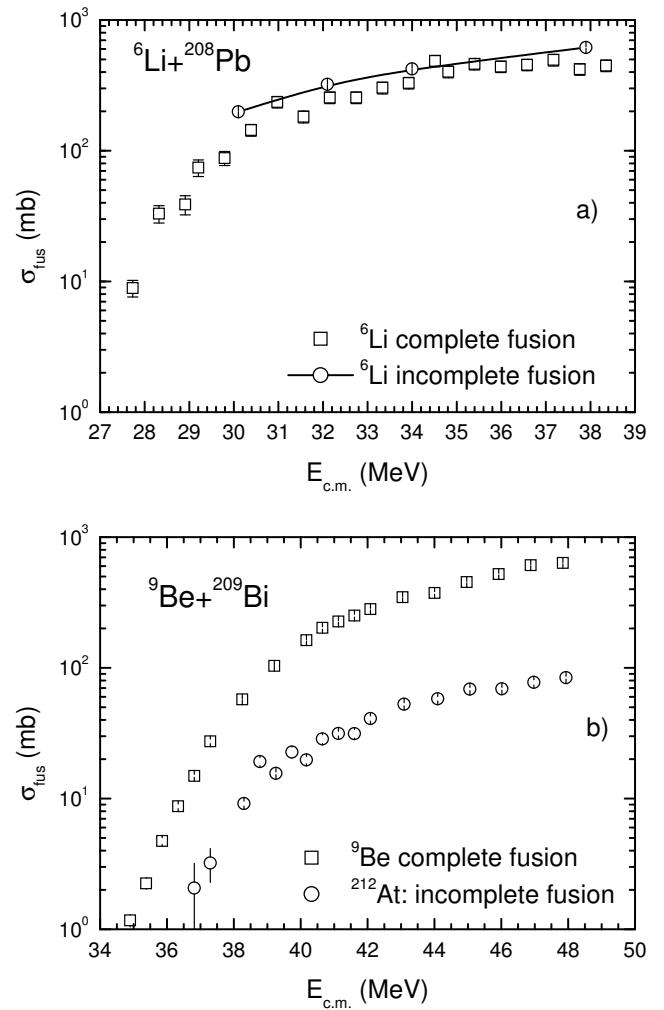


Fig. 1. a) Complete- and incomplete-fusion cross-sections for the system ${}^6\text{Li} + {}^{208}\text{Pb}$; b) Same as in a) but for the system ${}^9\text{Be} + {}^{209}\text{Bi}$.

3 Fusion data and analysis

It is well known that fusion near and below the Coulomb barrier is strongly affected [20] by the intrinsic degrees of freedom of the interacting nuclei, whose coupling with the relative motion causes an energy splitting of the single uncoupled fusion barrier. This gives rise to a distribution of barrier heights [21], that manifests itself as an enhancement of the fusion cross-sections at energies near and below the Coulomb barrier. Above the Coulomb barrier this effect becomes less important and, at energies well above the Coulomb barrier, it can be neglected. Fusion cross-section of tightly bound nuclei can be satisfactorily described with the semi-classical approach formula

$$\sigma_{fus}(E_{c.m.}) = \pi R_B^2 \left[1 - \frac{V_B}{E_{c.m.}} \right], \quad (3)$$

Table 2. The measured cross-sections for the system ${}^9\text{Be} + {}^{209}\text{Bi}$.

$E_{c.m.}$ (MeV)	$\sigma_{\text{ICF}}^{\text{exp.}}$ (mb)	$\Delta\sigma_{\text{ICF}}^{\text{exp.}}$ (mb)
36.335	0.78	0.40
36.815	2.07	1.13
37.294	3.22	0.93
38.301	9.15	0.39
38.780	19.2	1.36
39.259	15.6	0.36
39.734	22.7	2.12
40.170	19.7	1.26
40.650	28.6	2.19
41.129	31.4	1.29
41.608	31.4	2.35
42.088	41.0	1.80
43.094	52.7	1.48
44.101	58.1	2.33
45.060	68.8	1.92
46.018	69.2	1.78
46.977	77.4	3.56
47.936	84.1	2.07

where V_B (R_B) is the barrier height (radius). We can rewrite eq. (3) as

$$\frac{\sigma_{\text{fus}}(E_{c.m.}) E_{c.m.}}{\pi R_B^2} = E_{c.m.} - V_B. \quad (4)$$

The left-side term of eq. (4), called ‘‘reduced-fusion cross-section’’ $\sigma_{\text{fus}}^{\text{red}}$ (note that this is not a cross-section, but an energy), is a linear function of $E_{c.m.}$ if for σ_{fus} we assume the theoretical value from eq. (3).

For weakly bound nuclei, the situation is more complicated. Couplings to channels that act as doorways to breakup enhance the sub-barrier fusion cross-sections, whereas breakup itself may result in capture of only a part of the projectile, thus suppressing complete fusion. These two effects may either partially or totally cancel at energies below the barrier. Above the Coulomb barrier, however, the breakup-capture and/or stripping-like process may manifest itself as incomplete fusion due to the disappearance of the coupling effects. We will therefore discuss the effect of breakup on fusion by comparing experimental complete-fusion cross-sections to eq. (4). Figures 2a and b show the ‘‘reduced-fusion cross-section’’ for the four considered systems. The adopted barrier radius (R_B) and height (V_B) are listed in table 3. The corresponding barrier radii are calculated using the formula [22]

$$V_B = 1.44 \frac{Z_1 Z_2}{R_B} \left(1 - \frac{a}{R_B} \right), \quad (5)$$

where Z_1 , Z_2 are the atomic numbers of projectile and target nuclei, and $a = 0.65$ fm is the diffuseness parameter.

In the case of tightly bound nuclei, the breakup probability is always assumed to be very small. Hence, the effect of breakup on fusion should be weak. This is the case for the well-bound system ${}^{16}\text{O} + {}^{208}\text{Pb}$ [23] that, in the energy

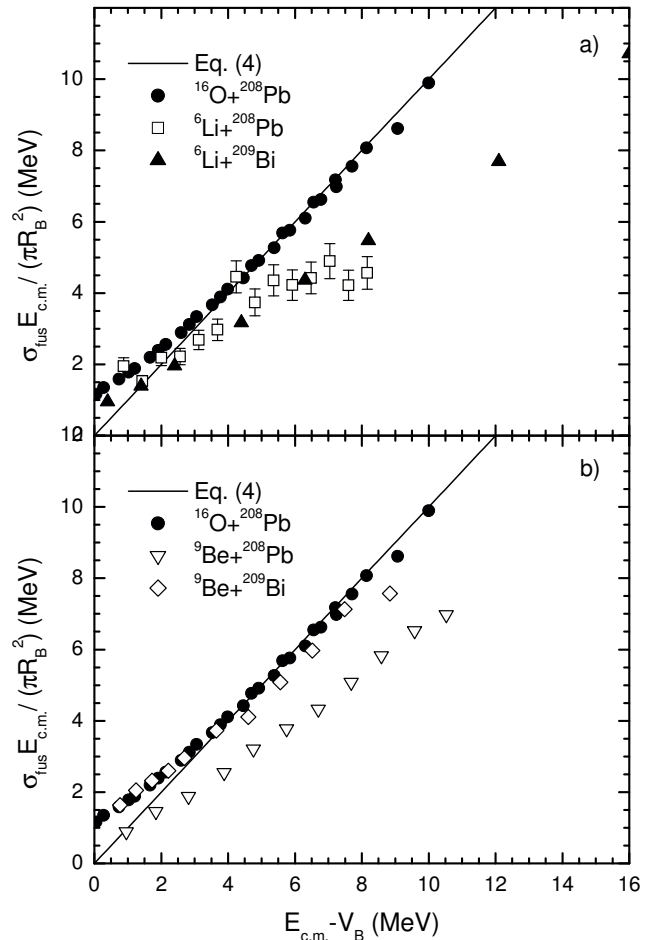


Fig. 2. a) Reduced-fusion cross-sections $\sigma_{\text{fus}}^{\text{red}}$ as a function of $(E_{c.m.} - V_B)$ for the systems ${}^6\text{Li} + {}^{208}\text{Pb}$, ${}^6\text{Li} + {}^{209}\text{Bi}$ and ${}^{16}\text{O} + {}^{208}\text{Pb}$. The solid straight line represents eq. (4). b) Same as in a) but for the systems ${}^9\text{Be} + {}^{208}\text{Pb}$, ${}^9\text{Be} + {}^{209}\text{Bi}$ and ${}^{16}\text{O} + {}^{208}\text{Pb}$.

Table 3. Fusion barrier parameters and the references where the barrier height V_B is quoted or extracted from the relevant data.

Reaction system	V_B (MeV)	R_B (fm)	Reference
${}^6\text{Li} + {}^{208}\text{Pb}$	30.1	11.00	[12]
${}^6\text{Li} + {}^{209}\text{Bi}$	30.6	11.01	[13]
${}^9\text{Be} + {}^{208}\text{Pb}$	38.3	11.28	[14]
${}^9\text{Be} + {}^{209}\text{Bi}$	39.4	11.30	[15]
${}^{16}\text{O} + {}^{208}\text{Pb}$	74.9	11.76	[23]

region above the barrier, follows rather well the straight line deduced from eq. (4), as shown in figs. 2a and b. Therefore, the ${}^{16}\text{O} + {}^{208}\text{Pb}$ system can be taken as a good reference for the discussion of breakup effects on fusion. In the case of the weakly bound projectile induced reactions ${}^6\text{Li} + {}^{208}\text{Pb}$, ${}^6\text{Li} + {}^{209}\text{Bi}$ and ${}^9\text{Be} + {}^{208}\text{Pb}$ [12–14], figs. 2a and b show that complete-fusion cross-sections lie below

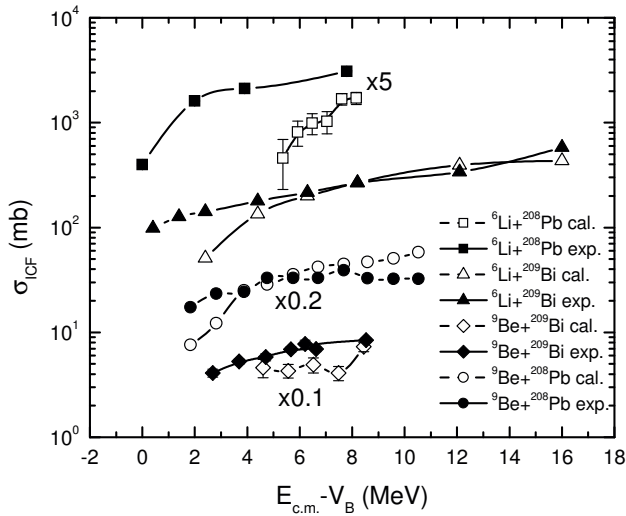


Fig. 3. The cross-sections of partial fusion as a function of $(E_{c.m.} - V_B)$ for the systems $^6\text{Li} + ^{208}\text{Pb}$, $^6\text{Li} + ^{209}\text{Bi}$, $^9\text{Be} + ^{208}\text{Pb}$ and $^9\text{Be} + ^{209}\text{Bi}$. The filled and open symbols show the measured and evaluated results, respectively.

the straight line at energies above the Coulomb barrier. For the system $^9\text{Be} + ^{209}\text{Bi}$ [15], the deviation from eq. (4) is very small compared to $^9\text{Be} + ^{208}\text{Pb}$. This different behavior, already pointed out in ref. [24], has not yet been fully understood. The analysis of fig. 2 shows that in all 4 cases there is some “missing” fusion cross-section (actually in the $^9\text{Be} + ^{209}\text{Bi}$ case, this is rather small), and we believe that this is most likely the incomplete-fusion one. The calculated and experimental σ_{ICF} are compared in fig. 3. The calculated ICF is the difference between the σ_{fus} given by eq. (4) and the experimental complete fusion. The ICF cross-sections for the systems $^6\text{Li} + ^{209}\text{Bi}$, $^9\text{Be} + ^{208}\text{Pb}$ and $^9\text{Be} + ^{209}\text{Bi}$ are in good agreement, although theoretical values tend to be smaller than experimental ones for the last system. This discrepancy becomes bigger if we remember that the $^9\text{Be} + ^{209}\text{Bi}$ σ_{ICF} in table 2 are σ_{ICF} lower limits. The best agreement is in the case of the $^9\text{Be} + ^{208}\text{Pb}$ and $^6\text{Li} + ^{209}\text{Bi}$ systems where the σ_{ICF} was evaluated from the cross-section of the populated evaporation residues, cases which can be clearly attributed to a partial-fusion process. For the system $^6\text{Li} + ^{208}\text{Pb}$ the partial-fusion cross-sections extracted from the breakup data are very different from those evaluated from the complete-fusion data. A possible explanation of such large discrepancy is that in the $^6\text{Li} + ^{208}\text{Pb}$ experiment we measured the cross-sections for the processes where one alpha (deuteron) is trapped into the target regardless of the detail of the “trapping”, in particular the kinematic one, and this cross-section was all attributed to ICF. It is possible that other reaction mechanisms in addition to “incomplete fusion” are contributing to this channel. To solve this problem, additional experiments with complete reconstruction of the 3-body kinematics might be necessary. This has been recently undertaken in the systems

$^6\text{Li} + ^{12}\text{C}$, ^{59}Co [25]. We can conclude that for all the cases considered in the present work:

- in the two cases $^6\text{Li} + ^{209}\text{Bi}$ and $^9\text{Be} + ^{208}\text{Pb}$, the CF and ICF are up to the total fusion so there is no connection originated from breakup;
- this is most likely not the case of $^9\text{Be} + ^{209}\text{Bi}$ since the experimental ICF is more than expected;
- the system $^6\text{Li} + ^{208}\text{Pb}$ is out of this schema since the “measured” ICF is much bigger than expected.

Recently, Diaz-Torres *et al.* [26] investigated the effect of breakup on total fusion for $^{6,7}\text{Li} + ^{209}\text{Bi}$ using a new continuum-discretized coupled-channel (CDCC) method. They found that the breakup enhances the total fusion at energies just around the barrier, whereas it hardly affects the total fusion at energies well above the barrier. Thus, their theoretical work supports our analysis of the $^6\text{Li} + ^{209}\text{Bi}$ system.

4 Conclusions

In summary, data on partial fusion for the systems $^6\text{Li} + ^{208}\text{Pb}$, $^9\text{Be} + ^{209}\text{Bi}$ have been evaluated. The effects of breakup on fusion for weakly bound projectiles ^6Li and ^9Be impinging on ^{208}Pb or ^{209}Bi targets have been investigated by comparing experimental fusion excitation functions to standard theory predictions. It results that complete fusion of a weakly bound projectile with heavy target is suppressed, whereas in most cases breakup has very little effect on the total fusion at energies above the barrier. The result indicates that partial fusion of weakly bound nuclei most likely takes place near the absorption region. Besides, in terms of the relationship between the σ_{CF} and σ_{ICF} , we have evaluated the cross-sections of partial fusion and compared them with the direct measured data.

This work was supported by the National Natural Science Foundation of China under Grant No. 10235030 and the Major State Basic Research Development Program under Grant No. G200007400.

References

- M.S. Hussein *et al.*, Phys. Rev. C **46**, 377 (1992); **47**, 2398 (1993).
- L.F. Canto *et al.*, Phys. Rev. C **52**, R2848 (1995).
- N. Takigawa *et al.*, Phys. Rev. C **47**, R2470 (1993).
- K. Yabana, Prog. Theor. Phys. **97**, 437 (1997).
- C.H. Dasso *et al.*, Phys. Rev. C **50**, R12 (1994).
- K. Hagino *et al.*, Phys. Rev. C **61**, 037602 (2000).
- J.J. Kolata *et al.*, Phys. Rev. Lett. **81**, 4580 (1998).
- M. Trotta *et al.*, Phys. Rev. Lett. **84**, 2342 (2000).
- A. Yoshida *et al.*, Phys. Lett. B **389**, 457 (1996).
- C. Signorini *et al.*, Eur. Phys. J. A **2**, 227 (1998).
- C. Signorini *et al.*, Nucl. Phys. A **735**, 329 (2004).
- Y.W. Wu *et al.*, Phys. Rev. C **68**, 044605 (2003).
- M. Dasgupta *et al.*, Phys. Rev. C **66**, R041602 (2002).
- M. Dasgupta *et al.*, Phys. Rev. Lett. **82**, 1395 (1999).

15. C. Signorini *et al.*, Eur. Phys. J. A **5**, 7 (1999).
16. K.E. Rehm *et al.*, Phys. Rev. Lett. **81**, 3341 (1998).
17. C. Beck *et al.*, Phys. Rev. C **67**, 054602 (2003).
18. C. Signorini *et al.*, Phys. Rev. C **67**, 044607 (2003).
19. G.F. Prete *et al.*, Nucl. Instrum. Methods Phys. Res. A **422**, 263 (1999).
20. M. Beckman, Rep. Prog. Phys. **51**, 1047 (1998) and references therein.
21. C.H. Dasso *et al.*, Nucl. Phys. A **405**, 381 (1992).
22. R.A. Broglia, A. Winther, *Heavy Ion Reactions* (Addison-Wesley, Redwood City, 1991) p. 116.
23. C.R. Morton *et al.*, Phys. Rev. C **60**, 044608 (1999).
24. C. Signorini *et al.*, Prog. Theor. Phys. Suppl. **154** (2004) 272.
25. A. Szanto de Toledo *et al.*, Nucl. Phys. A **734**, 311 (2004).
26. A. Diaz-Torres *et al.*, Phys. Rev. C **68**, 044607 (2003).